An Enzyme-Free Amperometric Sensor Based on Self-Assembling Ferrocene-Conjugated Oligopeptide for Specific Determination of L-Arginine

Zhu, Kai Jie; Zhou, Li; Wu, Ling; Feng, Sai Fei; Hu, Hui Ying; He, Jing Lin; He, Yu Min; Feng, Ze Meng; Yin, Yu Long; Yu, Donghong; Cao, Zhong

Published in:
Chinese Journal of Chemistry

DOI (link to publication from Publisher):
10.1002/cjoc.202100245

Publication date:
2021

Document Version
Accepted author manuscript, peer reviewed version

CJC Chinese Journal of Chemistry
中国化学 - An International Journal

Accepted Article

Title: An enzyme-free amperometric sensor based on self-assembling ferrocene-conjugated oligopeptide for specific determination of L-arginine

Authors: Kai-Jie Zhu, Li Zhou, Ling Wu*, Sai-Fei Feng, Hui-Ying Hu, Jing-Lin He, Yu-Min He, Ze-Meng Feng, Yu-Long Yin, Donghong Yu, Zhong Cao*

This work may now be cited as: *Chin. J. Chem.* **2021**, *39,* 10.1002/cjoc.202100245.

The final Version of Record (VoR) of it with formal page numbers will soon be published online in Early View: http://dx.doi.org/10.1002/cjoc.202100245.

WILEY-VCH SIOC CCS

ISSN 1001-604X • CN 31-1547/O6
mc.manuscriptcentral.com/cjoc
www.cjc.wiley-vch.de

Cao Zhong (Orcid ID: 0000-0001-8521-2552)

Cite this paper: *Chin. J. Chem.* **2021**, *39*, XXX—XXX. **DOI: 10.1002/cjoc.202100XXX**

An enzyme-free amperometric sensor based on self-assembling ferrocene-conjugated oligopeptide for specific determination of L-arginine

Kai-Jie Zhu[1,a], Li Zhou[1,a], Ling Wu*[,a], Sai-Fei Feng[a], Hui-Ying Hu[a], Jing-Lin He[a], Yu-Min He[b], Ze-Meng Feng[b], Yu-Long Yin[b], Donghong Yu[c], Zhong Cao*[,a]

[a] *Hunan Provincial Key Laboratory of Materials Protection for Electric Power and Transportation, and Hunan Provincial Key Laboratory of Cytochemistry, School of Chemistry and Biological Engineering, Changsha University of Science and Technology, Changsha 410114, China*
[b] *Institute of Subtropical Agriculture, Chinese Academy of Sciences, Changsha 410125, China*
[c] *Department of Chemistry and Bioscience, Aalborg University, DK-9220 Aalborg, East, Denmark*

Keywords

L-arginine | oligopeptide | conformational change | enzyme-free | amperometric sensor

Main observation and conclusion

An enzyme-free amperometric sensor based on a heptadecapeptide possessing an electroactive ferrocene (Fc) linker as ferrocene-Gly-Gly-Gly-Gly-Phe-Gly-His-Ile-His-Glu-Gly-Tyr-Gly-Gly-Gly-Gly-Lys-$(CH_2)_4$-dithiocyclopentane self-assembled on gold substrate was designed and fabricated for specific determination of L-arginine (L-Arg). The detection mechanism is based on conformational change of surface-immobilized peptide induced by the target L-Arg, which was confirmed via SEM, TEM, AFM, XPS, and SPR studies. The binding affinity and the recognition feasibility of immobilized specific and non-specific peptides were also assessed using electrochemical impedance spectroscopy (EIS), cyclic voltammetry (CV), and differential pulse voltammetry (DPV). The proposed method can serve as "signal-on" sensor for detection of L-Arg down to 31 pM with broad linear range (0.0001 to 10 μM). Furthermore, the Fc-conjugated specific peptide sensor was successfully applied to the determination of L-Arg in pig serums with a recovery rate of 97.5~106.9%, and its test results are in good agreement with that of chromatographic instrument, evidencing that the oligopeptide-based sensor can be served as a simple and enzyme-free biosensing platform towards L-Arg for future application.

Comprehensive Graphic Content

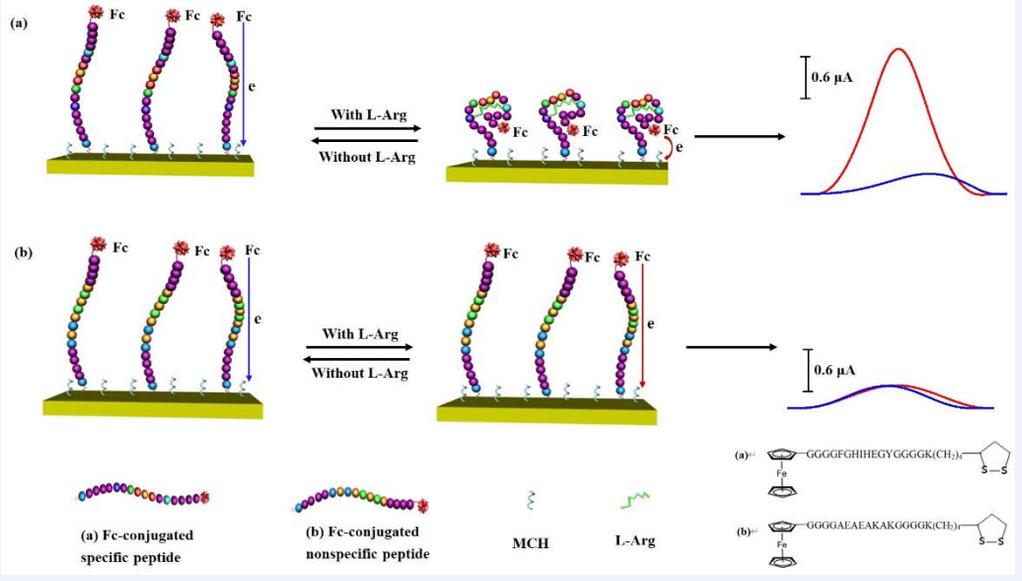

*E-mail: 152301006@csu.edu.cn (L. Wu), caoz@csust.edu.cn (Z. Cao)

Background and Originality Content

As elementary units of protein, amino acids are of great essential in maintaining specific physiological processes, participating in neuromodulation, and affecting organ function [1-2]. Being the most alkaline one, L-arginine (L-Arg) plays an important role in many biological functions, such as cell division, immune response, and wound healing [3-5]. Moreover, low levels of L-Arg have been found being related to tumors, which was a new organism formed by local tissue cell proliferation under the action of various tumorigenic factors. As one knows, the concentration of L-Arg in normal human plasma is about 90-150 μM, while representative plasma concentrations of arginine for patients with different types of cancer are: 76 ± 5 μM for pancreatic cancer, 80 ± 3 μM for breast cancer, and 42 ± 13 μM for esophageal cancer, which are all significantly lower than those of normal levels [6]. In addition, the content of L-Arg also affects the growth rate, nutritional status, and reproductive performance of animals like pig, fish, and sheep [7]. Therefore, it is crucial to develop a highly sensitive and selective assay for L-Arg in the fields of bioscience and health assessment.

Conventional techniques for the assay of L-Arg included high performance liquid chromatography (HPLC) [8], mass spectrometry (MS) [9], ion exchange paper chromatography [10], thin-layer chromatography [11], and high temperature paper chromatography [12], etc. However, these methods generally involve rigorous sample treatment, long analysis time, high cost, low sensitivity, and skilled operators. Recently, some alternative sensors for monitoring of L-Arg have been well established. For example, utilization of a functionalized UiO-67 metal–organic frameworks as a fluorescent sensor allowed for detection of arginine amino acid with the limit of detection of 17 nM [13]. Cao *et al*. designed a cationic dansyl derivative-based fluorescence probe and combined it with anionic surfactant assemblies and Cu^{2+} as a detector for the detection of arginine [14]. Via the electrostatic interaction between anionic surfactants and positively charged L-Arg target, a detection limit of 170 nM has been achieved. The level of arginine in real urine samples has been identified by inhibiting the growth of gold nanoparticles/carbon quantum dots composite using a bidimensional optical sensing combined with colorimetric and fluorometric [15]. Based on the unique guanidino group of arginine induced citrate-capped gold nanoparticles (AuNPs) aggregation at pH < pI, it has been conducted for visual detection of arginine [16]. Despite their numerous advantages, above methods involve either sophisticated synthesis steps, labeling, complicated modification of the nanoparticles, or strict test conditions. Therefore, it is still an important and challenging task to develop a simple, rapid, and accurate method for efficient and cost-effective detection of L-Arg.

With such advantages as convenient operation, good selectivity, high sensitivity, low cost, and environmental friendliness, electrochemical sensors have gained increased interests for detection of nitrogen-containing small molecules [17, 18]. Currently, electrochemical techniques for the assay of L-Arg were typically based on enzymatic biosensors [19-22], conducting polymers [23], molecularly imprinted polymers [24], and nanomaterials [25]. For example, double enzyme (arginase I and urease) and electroactive polyaniline (PANi) modified platinum electrode, was applied to the detection of L-Arg in wine and juice samples, and the detection limit of L-Arg was 38 μM [21]. The recombinant yeast cells that overproduce human liver arginase I were used for electroanalysis of L-Arg, exhibiting their good electrocatalytic activity towards L-Arg, and the detection limit of L-Arg was 85 μM [19]. In addition, the urease immobilized biosensor with an ion-selective field effect transistor (ISFET) as a transducer was constructed for sensitive determination of L-Arg with a linear range of 0.1~2.0 mM and a detection limit of 0.05 mM [26]. However, these enzyme-based sensors were expensive and chemically unstable, which limited their application. Therefore, it is necessary to establish highly sensitive, stable and specific enzyme-free electrochemical sensors to measure the content of L-Arg in bioscience fields.

Very recently, a chiral sensor with a Pr^{3+}: $CaTiO_3$@Ag@ L-cysteine ternary material has been realized for rapid sensing of L-arginine and D -arginine enantiomers in an electrochemical cell, but the detection limit of about 0.1 mM was still insufficient for real-sample measurement since arginine was expressed at micromolar or even lower levels in plasma [25]. Singh *et al*. fabricated a nanocomposite (PANI/MWCNTs/Fe_3O_4) film modified glassy carbon electrode for L-arginine in leukemic blood with the detection limit of 20 μM, and the response time was 20 s [23]. Roy *et al*. has reported an imprinted polymeric sensor for selective determination of zinc and arginine using the synthesized zinc–arginine imprinted polymer mixed with multi-walled carbon nanotubes modified platinum electrode, and the detection limit of 18 and 15 pg mL^{-1} can be achieved, respectively [24]. Despite of those advantages, electrochemical sensors by assembling electrode surfaces with electrocatalytically active materials, conducting polymers, or molecularly imprinted polymers were still lack of sufficient selectivity and often interfered by the ingredient of complex samples.

Interestingly, the oligopeptide is small in size and easy to synthesize in a cost-efficient manner, and its moiety recognizes its target analyte in a specific way to mimic hormone-receptor interactions compared to other biomolecules [27, 28]. Recently, some peptide-based sensors were reported to be used in the determination of biological species such as proteins [29], enzymes [30], bacterial [27], and metal ions [31], etc. However, as to small molecule amino acid, there were still really few reports on oligopeptide molecules used for specific recognition of L-Arg so far. In this work, we designed a ferrocene (Fc)-conjugated heptadecapeptide containing a sequence of FGHIHEGY as a specific recognizer for L-arginine, which was modified with dithiocyclopentane at the N-terminus and a Fc label at the C-terminus (Scheme 1). Via the specific interaction of L-Arg target and the electrode surface-modified Fc-conjugated oligopeptide, an ultralow detection limit of L-arginine can reach 31 pM. The presented novel enzyme-free amperometric sensor has been successfully applied to determination of L-Arg in pig serums which is comparable to that of an instrumental method, HPLC, indicating its potential application prospect in life science and animal nutrition fields.

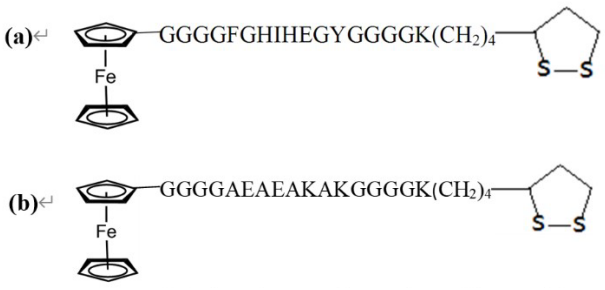

Scheme 1 Structure of designed Fc-conjugated specific peptide (a) and Fc-conjugated nonspecific peptide (b).

Results and Discussion

Design of Fc-peptide assembled sensor. Heptadecapeptides with various sequences were designed by our research group as shown in Scheme 1, in which the sequence of Fc-conjugated specific peptide for L-arginine is ferrocene-Gly-Gly-Gly-Gly-Phe

-Gly-His-Ile-His-Glu-Gly-Tyr-Gly-Gly-Gly-Gly-Lys-$(CH_2)_4$-dithiocyclopentane (Fc-GGGGFGHIHEGYGGGGK-C_4-DTCP). As control, other Fc-conjugated nonspecific peptide has a sequence of ferrocene-Gly-Gly-Gly-Gly-Ala-Glu-Ala-Glu-Ala-Lys-Ala-Lys-Gly-Gly-Gly-Gly-Lys $(CH_2)_4$-dithiocyclopentane (Fc-GGGGAEAEAKAKGGGGK-C_4-DTCP).

The Fc-conjugated peptide sequence as shown in Scheme 1 was designed to develop an functional peptide assembled amperometric biosensor for L-Arg detection based on the selectivity towards L-Arg, which was resulted from the eight amino acids with a sequence of FGHIHEGY as their corresponding binding sites. It is worth noting that the recognition sequence of FGHIHEGY for L-Arg has been successfully selected through scale simulate screening and further verified by isothermal titration calorimetry (ITC) [32, 33]. Ferrocene (Fc) was employed for ending group modification onto the peptide due to its good electrochemical properties and biocompatibility [34]. The presence of a dithiocyclopentanyl group in the Fc-conjugated specific peptide is conducive to provide a stable adhesion of peptide molecules onto the gold electrode via the Au–S bonding, avoiding the use of any other linking agents, and a spacer of -GGGGK- is used for keeping molecular flexibility on the gold surface. As a neutral thiol compound with a high affinity towards the Au surface, 6-mercapto-1-hexanol (MCH), is used to block macromolecular non-directional adsorption, as well as the use of aggregation inducers [35]. The specific recognition sequence at the middle part of the probe is responsible for the formation of arginine-peptide complex. The molecular recognition mechanism is based on conformational change of surface-immobilized peptide induced by the target L-Arg. As shown in Scheme 2, with introduction of L-Arg, the structure of the immobilized peptide probe is folded and assembled due to the formation of arginine-peptide complex, leading to a closer electron-transfer distance of Fc probe. Without the introduction of the target, the peptide is shown to partially foothold, thereby restricting electron transfer between the tethered Fc label and the electrode surface. Interestingly, the change in the electron- transfer distance of Fc probe is dependent on the target amino acid concentration, thus the sensor serves as a “signal-on” biosensing platform for specific detection of L-Arg.

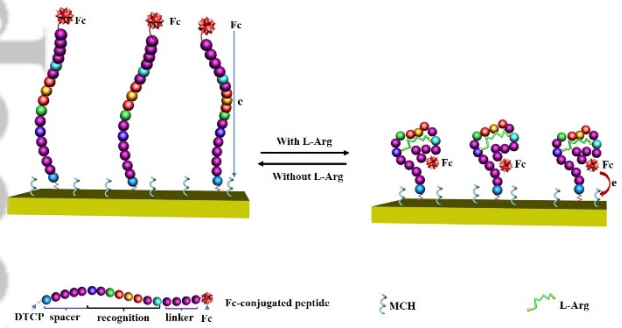

Scheme 2 Schematic diagram of the peptide-based amperometric biosensor binding with the target L-Arg. In the absence of L-Arg, the Fc-conjugated peptide is foothold and Fc current is low. Binding of L-Arg to the Fc-conjugated peptide induces a change in confromation leading to an increase in Fc current.

Characterization of sensing interface. Five important surface analysis techniques of scanning electron microscope (SEM), transmission electron microscope (TEM), atomic force microscopy (AFM), X-ray photoelectron spectroscopy (XPS), and surface plasmon resonance (SPR) were employed to confirm the surface immobilization and target recognition with the designed Fc-peptide on the gold substrate.

The micro-morphology of the Fc-conjugated specific peptide assembled on gold-coated silicon wafer was evaluated by SEM as

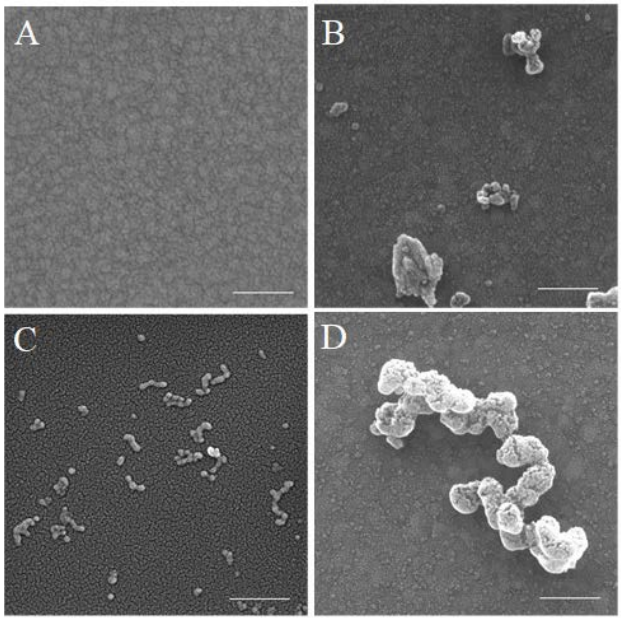

Figure 1 Characterization of Fc-conjugated specific peptide assembled film by using scanning electron microscopy. (A) Bare Au, (B) Fc-conjugated specific peptide/Au, (C) MCH/Fc-conjugated specific peptide/Au, (D) L-Arg/MCH/Fc-conjugated specific peptide/Au. Scale bar = 200 nm.

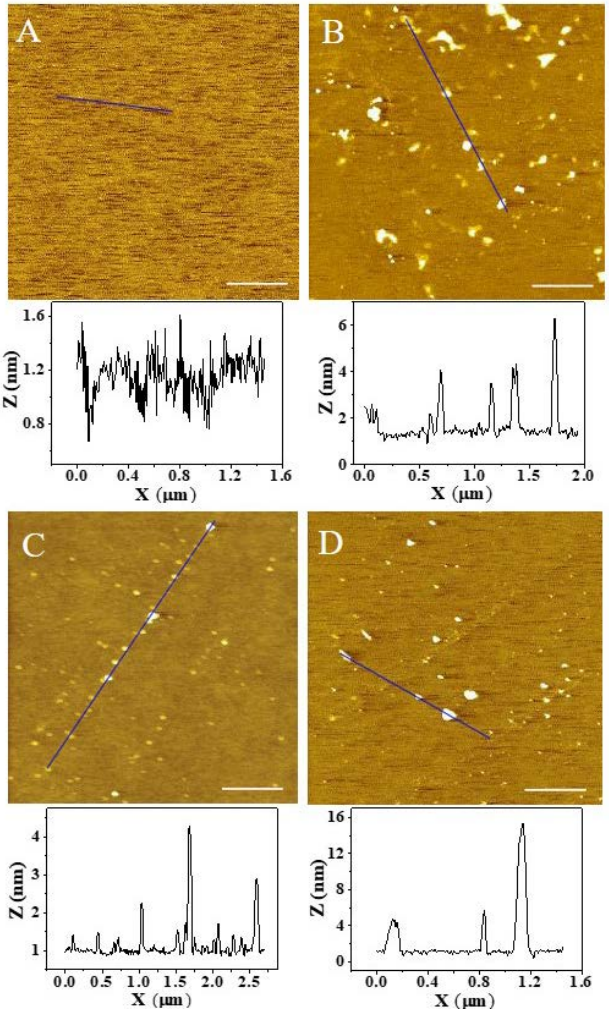

Figure 2 AFM topography (top) and cross-setion (bottom) of bare Au (A), Fc-conjugated specific peptide/Au (B), MCH/Fc-conjugated specific peptide/Au (C), and L-Arg/MCH/Fc-conjugated specific peptide/Au (D). Scale bar = 500 nm.

presented in Figure 1. There are no external substances adsorbed on the flat surface of the bare gold (Figure 1A), but some large agglomerates having diameter of 30~160 nm are formed on it after the assembly of Fc-conjugated specific peptide (Figure 1B). Interestingly, after incubation of the MCH onto the sensor interface, the large agglomerates are dispersed to form small cocoon-like particles in diameter of about 10~20 nm (Figure 1C) possibly due to the competitive displacement of the surface-modified peptide by imposed MCH. The addition of L-Arg significantly changes the morphology of the agglomerates on the gold surface (Figure 1D). The larger agglomerates might also be ascribed to the interaction between L-Arg and surface-immobilized peptide. These cocoon-like particles are regathered into larger aggregates of about 80~150 nm in diameter while combining with L-Arg.

Surprisingly, the TEM images further confirm that the changes in the morphology and structure of the Fc-conjugated specific peptide before and after the reaction with L-Arg in solution (Figure S1 in the Supporting Information). As shown in Figure S1, the Fc-conjugated specific peptide exhibits irregular macromolecular polypeptide (Figure S1A and corresponding enlarged Figure S1E). Upon the addition of L-Arg, an amount of target L-Arg are adsorbed on the surface of irregular macromolecular polypeptide via physical adsorption and specific binding (Figure S1B and corresponding enlarged Figure S1F). Interestingly, after the Fc-conjugated specific peptide probe mixed with MCH, the irregular macromolecular polypeptide is stretched to form a silk shape peptide oligomer by imposed MCH (Figure S1C and corresponding enlarged Figure S1G). Subsequently, after the incorporation of L-Arg into the resultant solution containing peptide and MCH, the peptide is folded and regathered into larger spherical agglomerates (Figure S1D and corresponding enlarged Figure S1H). Thus, the change in the morphology of the Fc-peptide before and after the addition of L-Arg is ascribed to the interaction between the Fc-conjugated specific peptide and L-Arg.

Subsequently, the stereo configurations of the particles were explored by AFM (Figure 2) which was used to picture the electrode surfaces and to compare the bare gold electrode surface to those with the different materials. Nanoscope Analysis 1.5 was used, as above-described, for generating images of the modified electrodes' surfaces. The cross section tool was used to measure height change along the line labeled in the images. The bare gold coated silicon wafer has a roughness factor of 0.14 nm, reflecting the average height of the surface layer (Figure 2A). When the Fc-conjugated specific peptide was immobilized on the gold substrate, some particles could be observed (Figure 2B), sufficiently illustrating the successful immobilization and agglomeration of Fc-conjugated specific peptide on the gold surface. It can be seen that the height of the spherical peptide assemblies is about 2.7~4.9 nm, and the width falls in 60~120 nm, which is consistent with that in SEM studies demonstrated in Figure 1B. At the same time, it is further known that the polymer is a spherical structure recessed in the middle, with increased specific surface area. As shown in Figure 2C, when the gold surface with agglomerates was immersed in MCH solution for a short period of time, the general sizes of aggregation of the particles became smaller, whereas the height and width of the particles are reduced to 0.9~3.9 nm and 40~70 nm, respectively. It shows that MCH mainly affects the width rather than the height of the assembled aggregates without configuration changes by keeping highly linear orientation. Such configuration with well directional arrangement promotes the interaction or intercontact between the Fc-conjugated specific peptide agglomerates and the target, providing much wider binding region. After addition of L-Arg, it was directed to contact the interface of MCH/Fc-conjugated specific peptide, resulting further grown particles about 60~160 nm wide and 4~15 nm high as appeared in Figure 2D. These results are consistent with that of SEM in Figure 1D, further illustrating the formation process and morphological changes of the oligopeptide composite assembled sensing-recognition interface.

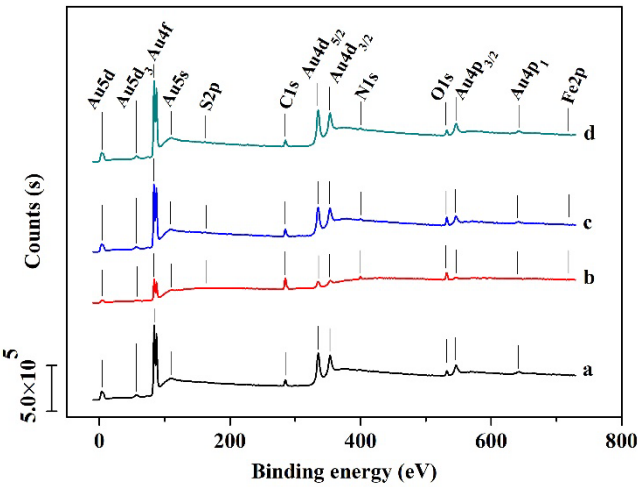

Figure 3 XPS spectra of bare Au (a), Fc-conjugated specific peptide/Au (b), MCH/Fc-conjugated specific peptide/Au (c), and L-Arg/MCH/Fc-conjugated specific peptide/Au (d). Figures S2(A~D) show the corresponding individual enlarged XPS spectra for (a), (b), (c), and (d).

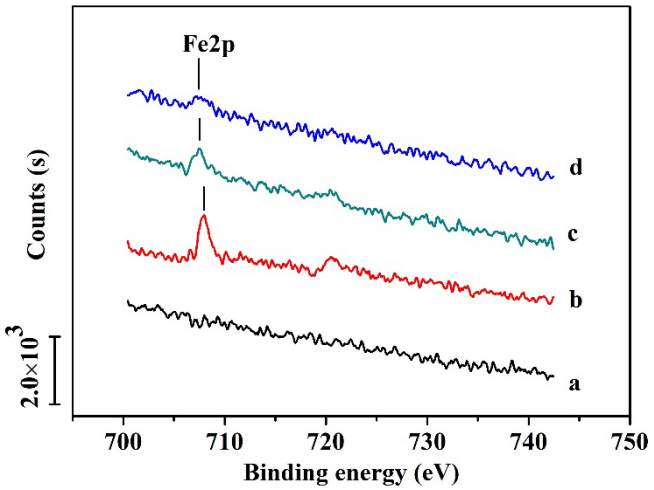

Figure 4 Averaged XPS elemental analysis from 10 scans of Fe2p for bare Au (a), Fc-conjugated specific peptide/Au (b), MCH/Fc-conjugated specific peptide /Au (c), and L-Arg/MCH/Fc-conjugated specific peptide /Au (d).

Table 1 Binding energy of C, O, N, S, and Fe for different composites

Electrode	Binding Energy (eV)					
	C1s	O1s	N1s	$S2p_{3/2}$	$S2p_{1/2}$	Fe2p
Bare Au	284.4	531.8	—	—	—	—
Fc-peptide/Au	284.5	531.6	399.9	161.9	163.2	708.0
MCH/Fc-peptide/Au	284.3	531.9	399.6	160.9	161.8	708.0
L-Arg/MCH/Fc-peptide/Au	284.4	531.5	399.5	160.9	161.8	707.5

Elemental analysis of the sensing interface can further prove that it is the Fc-conjugated specific peptide as the polymer that bound to the surface of the gold electrode instead of any other substance else. The changes were characterized by XPS for the elemental composition of different modified electrodes including bare Au (a), Fc-conjugated specific peptide/Au (b), MCH/Fc-conjugated specific peptide/Au (c), and L-Arg/MCH/Fc-conjugated specific peptide/Au (d) as shown in Figure 3. The presence of C, O,

N, S, and Fe peaks initially reveal that the modified surface contained the elementary composition of Fc-conjugated specific peptide, their corresponding binding energy data are listed in Table 1. Comparing with the bare Au (curve a), the distinct peaks of S2p at around 161.8 eV and N1s at around 399.6 eV for Fc-conjugated specific peptide/Au (b), MCH/Fc-conjugated specific peptide/Au (c), and L-Arg/MCH/Fc-conjugated specific peptide/Au (d) can be clearly seen from the corresponding individual enlarged XPS spectra as shown in Figures S2A~D in the Supporting Information, which is related to the formation of S-Au bond and the assembly of peptide [36], and a relatively strong peak of Fe2p at 706.7 eV for the modified electrode with respect to the bare Au is observed. Obviously, the averaged elemental analysis of XPS for Fe with 10 scans shows a more clearly peak at 706.7 eV only on the surface after Fc-conjugated specific peptide assembly (curves b, c, and d) as shown in Figure 4, indicating that the Fc-conjugated specific peptide containing Fe (II) is successfully immobilized on the surface and the peak of Fe2p is not brought about by any other substances.

On the other hand, when the Fc-conjugated specific peptide was incubated on the gold surface, the intensities of peaks of Au4f, Au5s, Au4d, and Au4p are significantly decreased (curve b) with respect to the bare Au (curve a) as seen from Figure 3. It is due to successful binding of the Fc-conjugated specific peptide to the gold substrate and also preventing the electrons of Au atom to escape outside becoming free electrons. When the MCH was bound to the Fc-conjugated specific peptide/Au interface, the intensities of the Au peaks are significantly increased on the contrary (curve c), indicating that the surface competitions between MCH and Fc-conjugated specific peptide lead to a certain amount of replacement of Fc-conjugated specific peptide by small MCH molecules, while the remaining Fc-conjugated specific peptide in less quantity still standing on the Au surface with well orientation with firmly sticking ability. These outcome from XPS study can also be proven by the above discussed AFM and SEM results.

Interestingly, the binding energy of oxygen for electrodes modified with different composites have been explored as 531.8, 531.6, 531.9, and 531.5 eV, respectively (Table 1). Obviously, the binding energy of O1s for the sensing interface of MCH/Fc-conjugated specific peptide/Au decreased 0.4 eV (from [illegible] eV to 531.5 eV) after contacting the target molecule of L-Arg, that is due to the electron cloud density of the oxygen increased leading to their increased electronegativity. This pronounces the interaction between binding sites on the specific sequence of oligopeptide chains and the target L-arginine, likewise via the weak hydrogen bonds of O—H···O and O—H···N. Unambiguous evidences for the L-Arg recognition process via SPR examination are revealed as shown in Figure S3, besides the above-mentioned SEM and AFM study.

Using SPR biosensors, the combination of Fc-conjugated specific peptide and L-Arg was investigated upon injection of different concentration of L-Arg on the Au sensor chips pre-immobilized with Fc-conjugated specific peptide and MCH (Figure S3). It can be clearly seen that the equilibrium analyses were in good agreement with the calibration curve. The MCH/Fc-conjugated specific peptide/Au responses to the injected L-Arg at a volume of 100 μL and flow rate of 40 μL/min. The changes in an SPR signal at equilibrium (Req) for the MCH/Fc-conjugated specific peptide/Au at L-Arg concentrations of 0.5, 1.0, and 10 μM were 1.29, 2.07, and 3.09 mDeg, respectively. From these results, the kinetic parameters k_d of (6.1 ± 0.1) × 10^{-4} s^{-1}, k_a of (8.1 ± 0.3) ×10^3 M^{-1} s^{-1}, and K_D of (75.4 ± 0.5) nM are obtained, and such a nanomolar K_D values indicates that the peptide aptamer has the strong binding capability to L-Arg. Therefore, the peptide aptamer-based sensor developed in this study is really specific for L-Arg.

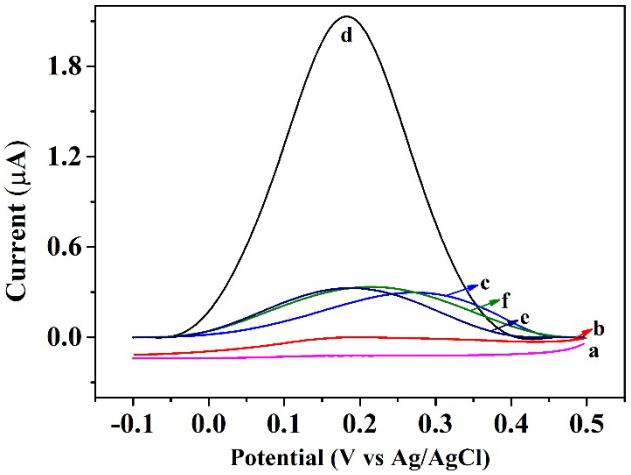

Figure 5 DPV curves of the bare Au electrode in 10 mM PBS buffer of pH 7.4 (a) and the buffer containing L-Arg (b). DPV curves of the MCH/Fc-conjugated specific peptide/Au in 10 mM PBS buffer of pH 7.4 (c) and the buffer containing L-Arg (d). DPV curves of the MCH/Fc-conjugated control peptide/Au in 10 mM PBS buffer of pH 7.4 (e) and the buffer containing L-Arg (f). The concentration of L-Arg is 1.0 μM.

Electrochemical characterization. The stepwise assembly of the gold electrode was characterized by using electrochemical impedance spectroscopy (EIS) and cyclic voltammetry (CV). As shown in Figure S4A in the Supporting Information, a pair of obviously reversible redox peaks at the bare gold surface is observed, suggesting a fast electron transfer (curve a). After assembling of the electrode with Fc-conjugated specific peptide, the corresponding peak currents become inconspicuous, which can be due to the nonconductive Fc-conjugated specific peptide bound to the modified electrode as an insulating film to inhibit electron transfer and hamper the redox probe of $[Fe(CN)_6]^{3-/4-}$ close to the gold surface (curve b). When the Fc-conjugated specific peptide modified electrode was further incubated with MCH (curve c), leading to a slight decreased in the peak currents which might be ascribed to the competitive displacement of the unspecific attachment of peptide probe by MCH. The results were further confirmed by EIS (Figure S4B). In comparison with the bare Au (R_{et}=0.32 kΩ, curve a), and that of the peptide after adsorption to the surface of the gold electrode exceeded R_{et} to 55 kΩ. Subsequently, blocking of the resultant electrode with MCH yields R_{et} of 46 kΩ. The EIS data are consistent with the CV results, indicating that the peptide was successfully immobilized on the gold surface through S-Au bonds, providing further evidence for the formation of an insulating peptide layer atop the gold surface.

The differential pulse voltammetry (DPV) behaviors of the bare Au and the MCH/Fc-conjugated specific peptide/Au electrodes in 10 mM PBS solution without or with 1.0 μM L-Arg were examined in detail (Figure 5). Seen from Figure 5, the bare Au electrode has no obvious redox peaks in either PBS (curve a) or L-Arg (curve b) solutions. Interestingly, there is a tiny reduction peak current at a potential of 0.28 V for the MCH/Fc-conjugated specific peptide/Au electrode in 10 mM PBS buffer of pH 7.4 without L-Arg (curve c), corresponding to the reduction of ferrocene of Fc-conjugated specific peptide. Upon the introduction of L-Arg (curve d), a much large reduction peak current was obtained at a potential of 0.18 V with 0.1 V decreased, indicating successful combination of L-Arg on the surface of Fc-conjugated specific peptide modified electrode. The increased current of curve d is ascribed to the formation of complex between L-Arg and 8-aa residues on the Fc-conjugated

specific peptide, which induces the folding of the peptide resulting in closer electron-transfer distance. As compared to the MCH/Fc-conjugated specific peptide/Au electrode, a similar reduction peak current in the case of PBS buffer (curve e) was obtained at the MCH/Fc-conjugated nonspecific peptide/Au electrode. After incorporation of L-Arg onto the MCH/Fc-conjugated nonspecific peptide/Au electrode, the reduction peak current in curve f was the same as that in curve e, suggesting that non-specific adsorption of L-Arg is negligible. Therefore, the Fc-conjugated specific peptide-based sensor can be served as an efficient way for specific recognition of the target L-Arg.

In summary, the interesting configuration of the Fc-conjugated specific peptide with middle-recessed spherical particles promotes the binding of the Fc-conjugated specific peptide to the target L-Arg, leading to highly selective detection of L-Arg from such Fc-conjugated specific peptide-based biosensor.

Effect on scan rates. The peak currents and potentials of MCH/ Fc-conjugated specific peptide/Au varied with different scan rates were examined by using cyclic voltammetry in 10 mM PBS (pH=7.4) containing 1.0 μM L-Arg (Figures S5A, B, and C). It can be seen that the reduction peak current is positively correlated with the scan rate and the linear regression equation can be fitted as I_{pa} = -0.02353v + 3.439 (R = 0.9988) (Figure S5B), which indicated an adsorption control process that the reduction peak of ferrocene on the surface of the restored modified electrode. As shown in Figure S5C, the reduction peak potential of ferrocene increases linearly with increasing logarithm of the scan rate, and the regression equation can be expressed as E_{pa} = 0.04815 lg$v$ + 0.3465 (R = 0.9972), theoretically corresponding to the Laviron equation [37] as follow:

$$E_{pa} = E^{0'} - \frac{2.303RT}{\alpha nF}\lg\frac{RTk^0}{\alpha nF} + \frac{2.303RT}{\alpha nF}\lg v \qquad (1)$$

where, E_{pa}, $E^{0'}$, α, n, T, R, F, k^0, v represent the oxidation peak potential, formula potential, electron transfer coefficient, electron transfer number, temperature, gas molar constant, Faraday constant, standard out-of-phase electron transfer rate constant, and scan rate, respectively. A value of $\alpha \cdot n$ = 0.52 was obtained by comparing with the above regression equation. Since the value of α is equal to 0.4~0.6 for irreversible electrode reactions, n=1 can be calculated accordingly. Therefore, it can be concluded that the number of electrons transferred during the reduction of ferrocene is about 1, and the number of transferred protons is also 1.

Analytical performance of the proposed biosensor for L-Arg. Under the optimal condition, the analytical performance of the proposed biosensor was evaluated by determining different concentrations of L-Arg samples with DPV (Figure 6). It can be seen that DPV peak current signals increased with the increasing concentration of L-Arg. The inset shows that this biosensor exhibited a wide linear range from 0.0001 to 10 μM with an ultra-low detection limit of 31 pM (S/N=3). The corresponding regression equation can be expressed as ΔI_{pa} = 0.2253 lgC + 3.014 (R = 0.9943). It is worth noting that the change of reduction peak current at each concentration was obtained by subtracting the background response, as depicted by curves f of Figure 5. Thus, quantitative determination of L-Arg levels in pig serum could be achieved with high specificity and selectivity.

Comparing the MCH/Fc-conjugated specific peptide/Au prepared herein with other analytical methods reported using different materials [16, 19-26, 38, 39] as shown in Table S1, it can be seen that the Fc-conjugated specific peptide biosensor in this work pronounces more excellent properties with lower detection limit,

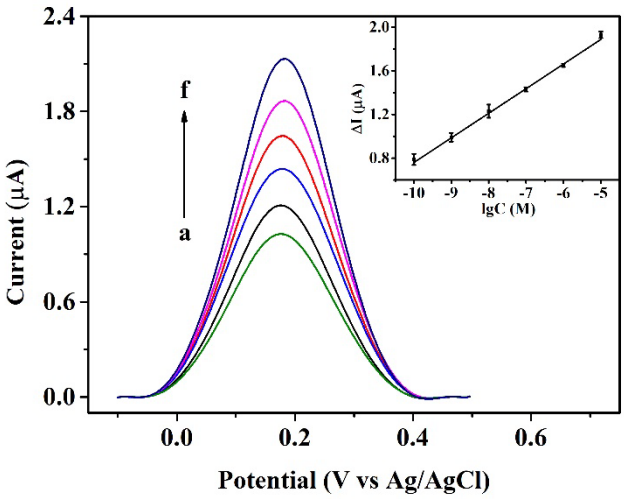

Figure 6 DPV response curves of MCH/Fc-conjugated specific peptide/Au in 10 mM PBS (pH=7.4) containing different concentrations of L-Arg. The inset shows a linear corresponding relationship between the background-subtracted reduction peak currents (ΔI_{pa}) and the concentrations of L-Arg. a→f: 0.0001, 0.001, 0.01, 0.1, 1.0, 10 μM.

especially than not only the spectrophotometry [16, 22] and fluorometry [22, 38, 39] but also the enzyme-based methods [19-23, 26].

Reproducibility, repeatability and stability. To evaluate the reproducibility of the proposed MCH/ Fc-conjugated peptide/Au, six different modified electrodes prepared under the same procedure condition were employed for parallel testing. The value of relative standard deviation (RSD) is 2.7% for 1.0 μM L-Arg by using the six electrodes, indicating that the Fc-peptide biosensor possesses good reproducibility. To evaluate the repeatability, six parallel experiments were performed in the presence of 1.0 μM L-Arg. The results show that the RSD value of the reduction peak currents is 2.3%, showing good repeatability. Moreover, the electrodes were freshly prepared and used for long-term monitoring in 1.0 μM L-Arg solution. The current responses of these electrodes for L-Arg remained 87% after one week, indicating that the stability of the electrode is good and acceptable.

Interference studies. To examine the sensor's anti-interference from coexisting substance with similar structure, other amino acids such as L-isoleucine (L-Ile), L-lysine (L-Lys), L-glycine (L-Gly), L-glutamic acid (L-Glu), L-histidine (L-His), L-phenylalanine (L-Phe), L-alanine (L-Ala), L-proline (L-Pro), L-threonine (L-Thr), L-glutamic Acid (L-Gln), L-valine (L-Val), L-tryptophan (L-Trp), L-tyrcsine (L-Tyr), L-aspartic acid (L-Asp), L-leucine (L-Leu), and L-methionine (L-Met) were test (Figure S6). It is apparent that the interferences caused by those 50-fold concentration amino acids are tiny or neglectable for L-Arg detection, while methionine serves as an S-containing amino acid that can be deposited on the gold electrode surface results in the current value decreased by 18%. In order to further eliminate the interference of the sensing system, the use of the MCH/ Fc-conjugated nonspecific peptide/Au electrode in case of L-Arg and 50-fold concentration of other amino acids mixture results in a negligible peak current, suggesting the coexisting substance does not interfere with L-Arg assay.

Analytical application with real sample detection. To verify the practical applicability of MCH/Fc-peptide/Au, the fabricated electrodes were used to detect L-Arg in real samples of pig serums and compared with commercial instruments such as the Agilent

1260 HPLC. As shown in Table 2, the results from the oligopeptide modified electrodes are consistent with those obtained by the HPLC method. Moreover, the recovery rates were found to be in the range from 97.5% to 106.9%, and the corresponding RSD is less than 4.6% (n = 5), demonstrating its applicable reliability. Therefore, this method can be well used for the quantitative determination of L-Arg in real serum samples.

Table 2 Determination of L-Arg in pig serums with corresponding recovery rate.

No.	HPLC (μM)	This method (μM)	RE (%)	Spiked (μM)	Found (μM)	Recovery (%)	RSD (%)
1	0.6278	0.6377	+1.6	0.2000	0.8285	100.3	3.4
2	0.9891	1.077	+8.9	0.2000	1.524	106.9	2.3
3	1.166	1.226	+5.2	0.2000	3.684	100.7	4.6
4	1.520	1.498	-1.4	0.2000	2.513	99.3	2.5
5	2.234	2.205	-1.2	0.2000	4.184	97.5	3.7

Conclusions

Based on the design of a ferrocene-linked heptadecapeptide assembling on gold surface, a novel enzyme-free amperometric biosensor was reported for specific and highly sensitive recognition of L-Arg, one type of conditionally essential amino acids. The self-assembly and binding process of immobilized synthetic peptides with or without L-Arg on the gold surface were characterized evidently. The high binding ability between the Fc-conjugated specific peptide sequence and L-Arg plays a key role in inducing the structure changes of the immobilized synthetic peptides, thereby forcing the distance of Fc probe close to the electrode surface. The biosensor has almost no interference from other common amino acids, due to the specific binding sites from the peptide to L-Arg only. It is worth mentioning that the oligopeptide based biosensor possesses excellent reproducibility, repeatability, stability, and ultralow limit (down to 31 pM) and satisfactory recoveries for detection of L-Arg in pig serums, announcing its important application prospects in life science and nutritional health.

Experimental

Fabrication of Fc-peptide electrodes. The Fc-conjugated specific peptide-modified gold electrode (Fc-conjugated specific peptide/Au) was prepared by immersing the cleaned bare Au in 10 mM phosphate buffer solution (PBS, pH=7.4) containing 40 μM of Fc-conjugated specific peptide and 50 mM of tris(carboxyethyl)phosphorus (TCEP) at 4 ℃ for 24 h in order to render the formation of a self-assembled Fc-conjugated specific peptide film on the Au surface. TCEP as a reducing agent is commonly used in biochemistry to reduce disulfide bonds of proteins and peptides in order to create Au-S bonding for Fc-conjugated specific peptide [40]. After the immobilization of Fc-conjugated specific peptide, the electrode was rinsed copiously with ultra-pure water and dried under dry N_2 stream. To block the unreacted gold surface and orient the Fc-conjugated specific peptide perpendicular to the surface, the Fc-conjugated specific peptide assembled electrode was soaked in a 1.0 mM MCH solution for 30 min. Finally, after being rinsed with 10 mM PBS and pure water, the MCH/Fc-conjugated specific peptide modified Au electrode was obtained, dried and stored at 4 ℃ prior to use. For comparison, the Fc-conjugated nonspecific peptide modified electrode was also fabricated following the above-mentioned procedure.

Measurement of pig serum samples. All pig serums were obtained from Institute of Subtropical Agriculture, Chinese Academy of Sciences (Changsha, China), and approved by the Animal Care and Use Committee of Changsha University of Science and Technology. The collection and use of pig serums follows the procedures previously reported by our group [17]. The content of L-Arg in pig serums were determined using the modified electrode and a commercially available HPLC instrument. The procedure for HPLC analysis of L-Arg in pig serums were in accordance with the previously reported [17].

Supporting Information

The supporting information for this article is available on the WWW under https://doi.org/10.1002/cjoc.2021xxxxx.

Acknowledgement

This work was financially supported by the projects of National Natural Science Foundation of China (31527803, 21545010, 21275022 and 21605009) and Natural Science Foundation of Hunan Province, China (2020JJ4599, 2019JJ50651).

References

[1] Verma, N.; Singh, A. K.; Singh, M. L-arginine biosensors: A comprehensive review. *Biochem. Biophys. Rep.* **2017**, *12*, 228-239.
[2] Coman, D.; Yaplito-Lee, J.; Boneh, A. New indications and controversies in arginine therapy. *Clin. Nutr.* **2008**, *27*, 489-496.
[3] Guelzim, N.; Mariotti, F.; Martin, P. G.; Lasserre, F.; Pineau, T.; Hermier, D. A role for PPARalpha in the regulation of arginine metabolism and nitric oxide synthesis. *Amino Acids* **2011**, *41*, 969-979.
[4] Vermeulen, M. A.; van de Poll, M. C.; Ligthart-Melis, G. C.; Dejong, C. H.; van den Tol, M. P.; Boelens, P. G.; van Leeuwen, P. A. Specific amino acids in the critically ill patient--exogenous glutamine/arginine: a common denominator? *Crit. Care Med.* **2007**, *35*, S568-S576.
[5] Stechmiller, J. K.; Childress, B.; Cowan, L. Arginine supplementation and wound healing. *Nutr. Clin. Pract.* **2005**, *20*, 52-61.
[6] Vissers, L. Y.; Dejong, C. H.; Luiking, Y. C.; Fearon, K. C. Plasma arginine concentrations are reduced in cancer patients: evidence for arginine deficiency? *Am. J. Clin. Nutr.* **2005**, *81*, 1142-1146.
[7] Lassala, A.; Bazer, F. W.; Cudd, T. A.; Datta, S.; Keisler, D. H.; Satterfield, M. C.; Spencer, T. E.; Wu, G. Parenteral administration of L-arginine enhances fetal survival and growth in sheep carrying multiple fetuses. *J. Nutr.* **2011**, *141*, 849-855.
[8] Chen, B. M.; Xia, L. W.; Liang, S. X.; Chen, G. H.; Deng, F. L.; R., Z. W.; Tao, L. J. Simultaneous determination of L-arginine and dimethylarginines in human urine by high-performance liquid chromatography. *Anal. Chim. Acta* **2001**, *444*, 223-227.
[9] Yu, X.; Yao, Z. P. Chiral differentiation of amino acids through binuclear copper bound tetramers by ion mobility mass spectrometry. *Anal. Chim. Acta* **2017**, *981*, 62-70.
[10] (15) Roberts, H. R.; Kolor, M. G. Rapid quantitative determination of arginine, histidine, and lysine by ion exchange paper chromatography. *Anal. Chem.* **1959**, *31*, 565-566.
[11] Bahl, S.; Naqvi, S.; Venkitasubramanian, T. A. Simple, rapid quantitative determination of lysine and arginine by thin-layer chromatography. *J. Agric. Food Chem.* **1976**, *24*, 56-59.
[12] Sibalic, S. M.; Radej, N. V. Determination of lysine, arginine, and histidine by high temperature paper chromatography. *Anal. Chem.* **1962**, *33*, 1223-1224.
[13] Mohammadi, L.; Khavasi, H. R. Anthracene-tagged UiO-67-MOF-mof as highly selective aqueous sensor for nanoscale detection of arginine

amino acid. *Inorg. Chem.* **2020**, *58*, 13091-13097.
[14] Cao, J.; Ding, L.; Hu, W.; Chen, X.; Chen, X.; Fang, Y. Ternary system based on fluorophore−surfactant assemblies Cu^{2+} for highly sensitive and selective detection of arginine in aqueous solution. *Langmuir* **2014**, *30*, 15364-15372.
[15] Liu, T.; Li, N.; Dong, J. X.; Zhang, Y.; Fan, Y. Z.; Lin, S. M.; Luo, H. Q.; Li, N. B. A colorimetric and fluorometric dual-signal sensor for arginine detection by inhibiting the growth of gold nanoparticles/carbon quantum dots composite. *Biosens. Bioelectron.* **2017**, *87*, 772-778.
[16] Pu, W.; Zhao, H.; Huang, C.; Wu, L.; Xu, D. Visual detection of arginine based on the unique guanidino group-induced aggregation of gold nanoparticles. *Anal. Chim. Acta* **2013**, *764*, 78-83.
[17] Zhu, Q.; Liu, C.; Zhou, L.; Wu, L.; Bian, K.; Zeng, J.; Wang, J.; Feng, Z.; Yin, Y.; Cao, Z. Highly sensitive determination of L-tyrosine in pig serum based on ultrathin CuS nanosheets composite electrode. *Biosens. Bioelectron.* **2019**, *140*, 111356.
[18] Li, Y. Q.; Zhu, Q.; Xiao, Z. L.; Lv, C. Z.; Feng, Z. M.; Yin, Y. L.; Cao, Z. Graphene oxide/triangular gold nanoplates/nafion composite modified electrode used for sensitive detection of L-tryptophan. *Chem. J. Chinese Univ.* **2018**, *39*, 636-644.
[19] Stasyuk, N. Y.; Gayda, G. Z.; Gonchar, M. V. L-Arginine-selective microbial amperometric sensor based on recombinant yeast cells over-producing human liver arginase I. *Sens. Actuators B-Chem.* **2014**, *204*, 515-521.
[20] Zhybak, M. T.; Fayura, L. Y.; Boretsky, Y. R.; Gonchar, M. V.; Sibirny, A. A.; Dempsey, E.; Turner, A. P. F.; Korpan, Y. I. Amperometric L-arginine biosensor based on a novel recombinant arginine deiminase. *Microchim. Acta* **2017**, *184*, 2679-2686.
[21] Stasyuk, N.; Smutok, O.; Gayda, G.; Vus, B.; Koval'chuk, Y.; Gonchar, M. Bi-enzyme L-arginine-selective amperometric biosensor based on ammonium-sensing polyaniline-modified electrode. *Biosens. Bioelectron.* **2012**, *37*, 46-52.
[22] Stasyuk, N. Y.; Gayda, G. Z.; Fayura, L. R.; Boretskyy, Y. R.; Gonchar, M. V.; Sibirny, A. A. Novel arginine deiminase-based method to assay L-arginine in beverages. *Food Chem.* **2016**, *201*, 320-6.
[23] Singh, A. K.; Sharma, R.; Singh, M.; Verma, N. Electrochemical determination of L-arginine in leukemic blood samples based on a polyaniline-multiwalled carbon nanotube-magnetite nanocomposite film modified glassy carbon electrode. *Instrum. Sci. Technol.* **2020**, *48*, 400-416.
[24] Roy, E.; Patra, S.; Madhuri, R.; Sharma, P. K. Development of an imprinted polymeric sensor with dual sensing property for trace level estimation of zinc and arginine. *Mater. Sci. Eng. C.* **2015**, *49*, 25-33.
[25] Zhang, W.; Li, J.; Lu, G.; Guan, H.; Hao, L. Enantiomer-selective sensing and the light response of chiral molecules coated with a persistent luminescent material. *Chem. Commun.* **2019**, *55*, 13390-13393.
[26] Sheliakina, M.; Arkhypova, V.; Soldatkin, O.; Saiapina, O.; Akata, B.; Dzyadevych, S. Urease-based ISFET biosensor for arginine determination. *Talanta* **2014**, *121*, 18-23.
[27] Chu, J.; Vila-Farres, X.; Brady, S. F. Bioactive synthetic-bioinformatic natural product cyclic peptides inspired by nonribosomal peptide synthetase gene clusters from the human microbiome. *J. Am. Chem. Soc.* **2019**, *141*, 15737-15741.
[28] Pavan, S.; Berti, F. Short peptides as biosensor transducers. *Anal. Bioanal. Chem.* **2012**, *402*, 3055-3070.
[29] Wu, L.; Hu, Y.; He, Y.; Xia, Y.; Lu, H.; Cao, Z.; Yi, X.; Wang, J. Dual-channel surface plasmon resonance monitoring of intracellular levels of the p53-MDM2 complex and caspase-3 induced by MDM2 antagonist Nutlin-3. *Analyst* **2019**, *144*, 3959-3966.
[30] Zhang, D.; Meng, Y. R.; Zhang, C. Y. Peptide-templated gold nanoparticle nanosensor for simultaneous detection of multiple posttranslational modification enzymes. *Chem. Commun.* **2019**, *56*, 213-216.
[31] Lotfi Zadeh Zhad, H. R.; Lai, R. Y. Application of calcium-binding motif of E-cadherin for electrochemical detection of Pb(II). *Anal. Chem.* **2018**, *90*, 6519-6525.
[32] Cao, Z; Zhou, L.; Zhu, K. J.; Zhu, Q.; He, J. L.; Xiao, Z. L.; He, Y.; Feng, Z.; Yin, Y. Method and sensor for detecting L-arginine based on peptide composite, CN Patent, Appl No.201910605833.3, **2019** 7. 5.
[33] He, Y.; Zhou, L.; Deng, L.; Feng, Z.; Cao, Z.; Yin, Y. An electrochemical impedimetric sensing platform based on a peptide aptamer identified by high-throughput molecular docking for sensitive l-arginine detection. *Bioelectrochemistry* **2021**, *137*, 107634.
[34] Li, Y.; Afrasiabi, R.; Fathi, F.; Wang, N.; Xiang, C.; Love, R.; She, Z.; Kraatz, H. B. Impedance based detection of pathogenic E. coli O157:H7 using a ferrocene-antimicrobial peptide modified biosensor. *Biosens. Bioelectron.* **2014**, *58*, 193-199.
[35] Bi, J.; Li, T.; Ren, H.; Ling, R.; Wu, Z.; Qin, W. Capillary electrophoretic determination of heavy-metal ions using 11-mercaptoundecanoic acid and 6-mercapto-1-hexanol co-functionalized gold nanoparticle as colorimetric probe. *J. Chromatogr. A* **2019**, *1594*, 208-215.
[36] Mihailescu, M.; Sorci, M.; Seckute, J.; Silin, V. I.; Hammer, J.; Perrin, B. S., Jr.; Hernandez, J. I.; Smajic, N.; Shrestha, A.; Bogardus, K. A.; Greenwood, A. I.; Fu, R.; Blazyk, J.; Pastor, R. W.; Nicholson, L. K.; Belfort, G.; Cotten, M. L. Structure and function in antimicrobial piscidins: histidine position, directionality of membrane insertion, and pH-dependent permeabilization. *J. Am. Chem. Soc.* **2019**, *141*, 9837-9853.
[37] Laviron, E. General expression of the linear potential sweep voltammogram in the case of diffusionless electrochemical systems. *J. Electroanal. Chem.* **1979**, 19-28.
[38] Ding, H. C.; Li, B. Q.; Pu, S. Z.; Liu, G.; Jia, D. C.; Zhou, Y. A fluorescent sensor based on a diarylethene-rhodamine derivative for sequentially detecting Cu^{2+} and arginine and its application in keypad lock. *Sens. Actuators B-Chem.* **2017**, *247*, 26-35.
[39] Pettiwala, A. M.; Singh, P. K. Supramolecular dye aggregate assembly enables ratiometric detection and discrimination of lysine and arginine in aqueous solution. *ACS Omega* **2017**, *2*, 8779-8787.
[40] Gomes, S. Q.; Vitoriano, L.; de Arruda, E. G. R.; Ruiz, A.; Candido, T.; de Carvalho, J. E.; Lustri, W. R.; Abbehausen, C. Linear gold(I) complex with tris-(2-carboxyethyl)phosphine (TCEP): selective antitumor activity and inertness toward sulfur proteins. *J. Inorg. Biochem.* **2018**, *186*, 104-115.

Manuscript received: XXXX, 2021
Manuscript revised: XXXX, 2021
Manuscript accepted: XXXX, 2021
Accepted manuscript online: XXXX, 2021
Version of record online: XXXX, 2021

Entry for the Table of Contents

An enzyme-free amperometric sensor based on self-assembling ferrocene-conjugated oligopeptide for specific determination of L-arginine

Kai-Jie Zhu[1,a], Li Zhou[1,a], Ling Wu*[,a], Sai-Fei Feng[a], Hui-Ying Hu[a], Jing-Lin He[a], Yu-Min He[b], Ze-Meng Feng[b], Yu-Long Yin[b], Donghong Yu[c], Zhong Cao*[,a]

Chin. J. Chem. **2021**, *39*, XXX—XXX. **DOI: 10.1002/cjoc.202100XXX**

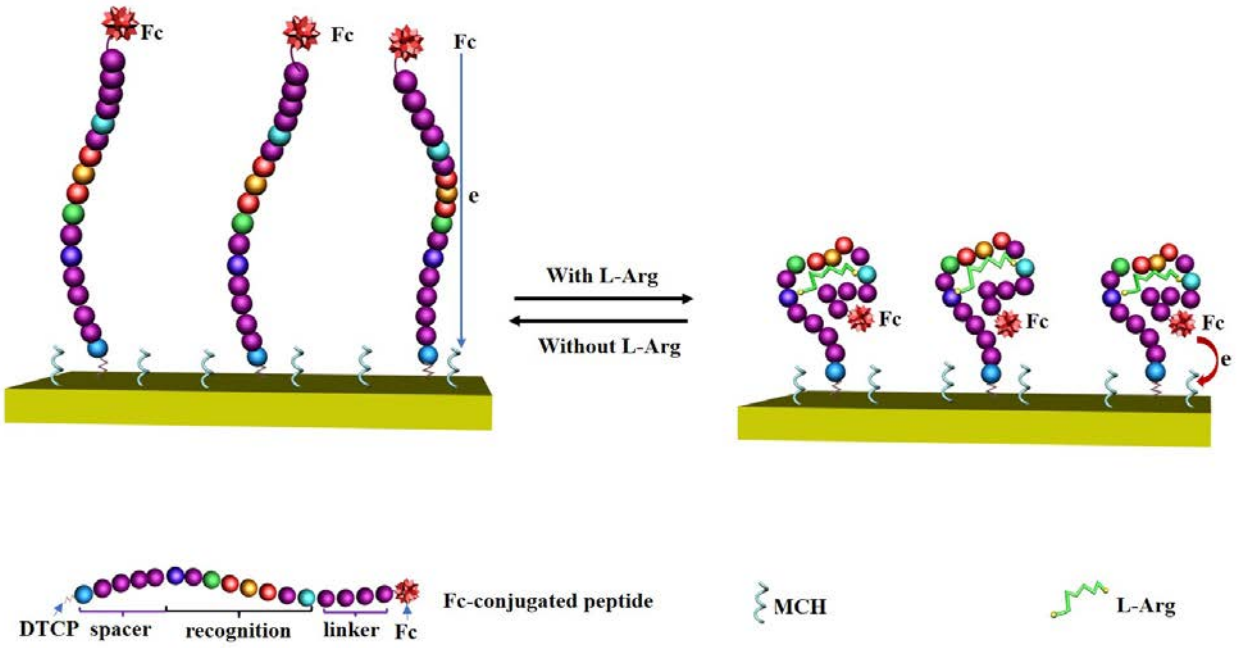

An enzyme-free amperometric sensor based on a Fc-conjugated specific peptide self-assembling on gold surface is proposed for highly selective detection of L-arginine. The sensing mechanism is based on the specific interaction between L-arginine and surface-immobilized peptide, which induces the change in conformation of peptide probe resulting in the electrochemical signal generation. The novel sensing protocol serves as a simple and enzyme-free biosensing platform for specific detection of L-Arg in future applications.